Forsmark site investigation

Mapping of borehole breakouts KFM08D

Processing of acoustical televiewer data from 2007 and 2014

Jørgen Ringgaard, Gert Andersen, Uffe Torben Nielsen

Rambøll Danmark A/S

April 2014

SKB

Forsmark site investigation

Mapping of borehole breakouts KFM08D

Processing of acoustical televiewer data from 2007 and 2014

Jørgen Ringgaard, Gert Andersen, Uffe Torben Nielsen

Rambøll Danmark A/S

April 2014

Abstract

This report presents a detection and mapping of borehole breakouts and other borehole deformations by means of processing of data from an acoustical televiewer probe. Special attention is paid to small breakouts and micro fallouts. The report included the results obtained in borehole KFM08D recorded in 2007 and 2014.

The registration is done in Excel-sheets in a table and a chart, which show the main azimuth of the breakouts. Due to the inclination of the boreholes, the televiewer is slightly decentralized during logging, which causes reduced data quality. But despite this, breakouts, keyseats and washouts with a certain magnitude (more than 0.1 mm), can still be mapped and classified after centralization of data by special processing routines.

Also micro fallouts (fallouts smaller than 0.1 mm) can be registered, but the mapping of these is more uncertain, as is it not possible to make specific criteria for this phenomenon. The detection has been done as a visual inspection and it is often hard to determine the area of distribution of these small structures. In some cases the micro fallouts are found to be in the entire perimeter of the borehole, but in other cases they have a main azimuth in the same direction as the breakouts.

Sammanfattning

Denna rapport redovisar resultaten från kartering av borrhålsspjälkning och andra deformationer i det djupa kärnborrhålet KFM08D i Forsmark, baserat på data från loggning med akustisk televiewer. Särskild vikt har lagts vid små borrhålsspjälkningar och mikroutfall. Rapporten inkluderar resultat från två loggningar med akustisk televiewer, den första utförd 2007 och den andra 2014. I rapporten ingår de resultat som erhållits i borrhål KFM08D under 2007 och 2014.

Dataregistreringen är utförd i Excel-blad i tabeller och diagram, vilka illustrerar huvud-azimuth för spjälkningarna. På grund av borrhålens lutning är televiewersonden svagt decentraliserad under loggningen, vilket leder till sämre datakvalitet. Trots detta är det möjligt att urskilja spjälkning, keyseats och washouts med bestämd magnitud (mer än 0,1 mm). Detta kan åstadkommas genom att centralisering kan göras genom en speciell dataprocessrutin.

Även mikroutfall (utfall mindre än 0,1 mm) kan urskiljas, men karteringen av dessa är mer osäker, då det inte är möjligt att precisera kriterium för detta. Identifiering har kunnat göras genom visuell bedömning, men ofta är det svårt att avgöra utbredningen av dessa. I några fall förekommer mikroutfall längs borrhålets hela perimeter, men i andra fall har de huvudazimuth i samma riktning som spjälkningen.

Contents

1 Introduction

This report presents results from mapping of borehole breakouts and other borehole deformations in the deep core drilled borehole KFM08D at Forsmark, Sweden, by means of processing of data from an acoustical televiewer probe. The report includes results obtained from loggings performed in 2007 and 2014.

Boreholes and tunnels in sedimentary formations as well as well as in hard crystalline bedrock may, during certain conditions governed by the relation between the compressive strength of the rock material and the state of stress, be exposed to spalling, often referred to as borehole breakouts, entailing that the originally circular borehole perimeter is deformed and changes its geometry to a more or less oval shape. (More exact definitions and a classification of borehole deformations of different types are given in Section 6.1.) The orientation of breakouts is governed by the stress field, such that the breakouts (ideally) occur on opposite sides of the borehole in the same bearing as that of the minor horizontal stress.

Width, length and depth of breakouts may vary within broad ranges, reflecting variations in the rock strength-/rock stress relation (Zoback et al. 1985) and possibly also mirroring the impact of the drilling process (Ask et al. 2006). The study of breakouts is primarily aiming at shedding light on the orientation of the stress field and its continuity. Secondarily, breakouts may be used also for determination of stress magnitudes, however mainly as a supporting method.

It has previously been shown that spalling phenomena may well be identified and characterized by the analysis of acoustic televiewer images (e.g. Deltombe and Schepers 2000. Due to the high accuracy of the acoustic televiewer method for determination of geometrical properties of the borehole, it is especially advantageous when addressing minor deformations, which may be very difficult to detect with other methods.

A pilot study aiming at investigating the potential of the acoustic televiewer method of identifying and characterizing major as well as minor borehole deformations in the rock types prevailing at Forsmark was performed during 2005 (Ask and Ask 2007, Ask et al. 2006). Two subvertical core drilled boreholes, KFM01A (1,000 m long) and KFM01B (500 m) were investigated. The applicability of the method was clearly demonstrated and a range of borehole deformations of different dimensions was revealed in both boreholes. A pilot study was also performed by Ringgaard (2007).

According to the theory for the generation of borehole breakouts, some degree of time dependence may be inherent in the process. In other words, the areal extension and amplitude of breakouts as well as their frequency in a specific borehole may, theoretically, increase versus the elapsed time after completion of drilling, until the stress field around the borehole has stabilized and steady-state conditions have been obtained. The degree of time dependence is due to several factors. In order to study this effect, two acoustical televiewer loggings with a time span of approximately 7 years have been performed in borehole KFM08D. By analysis of the results of the two surveys, conclusions are drawn whether the breakout generating process has been active during drilling completion and the first televiewer logging in February 2007, and between this logging and the second televiewer logging performed in January 2014, respectively.

This document reports the results gained by processing and interpretation of acoustic televiewer data from borehole KFM08D at Forsmark. The work was carried out in accordance with activity plan AP SFK-10-069, see Table 1-1.

A map of the borehole location at Forsmark investigation area is presented in Figure 1-1.

Table 1-1. Controlling document for performance of the activity.

Activity plan	Number	Version
Logging with acoustical televiewer and borehole deviation measurements with two methods	AP SFK-10-069	0.1
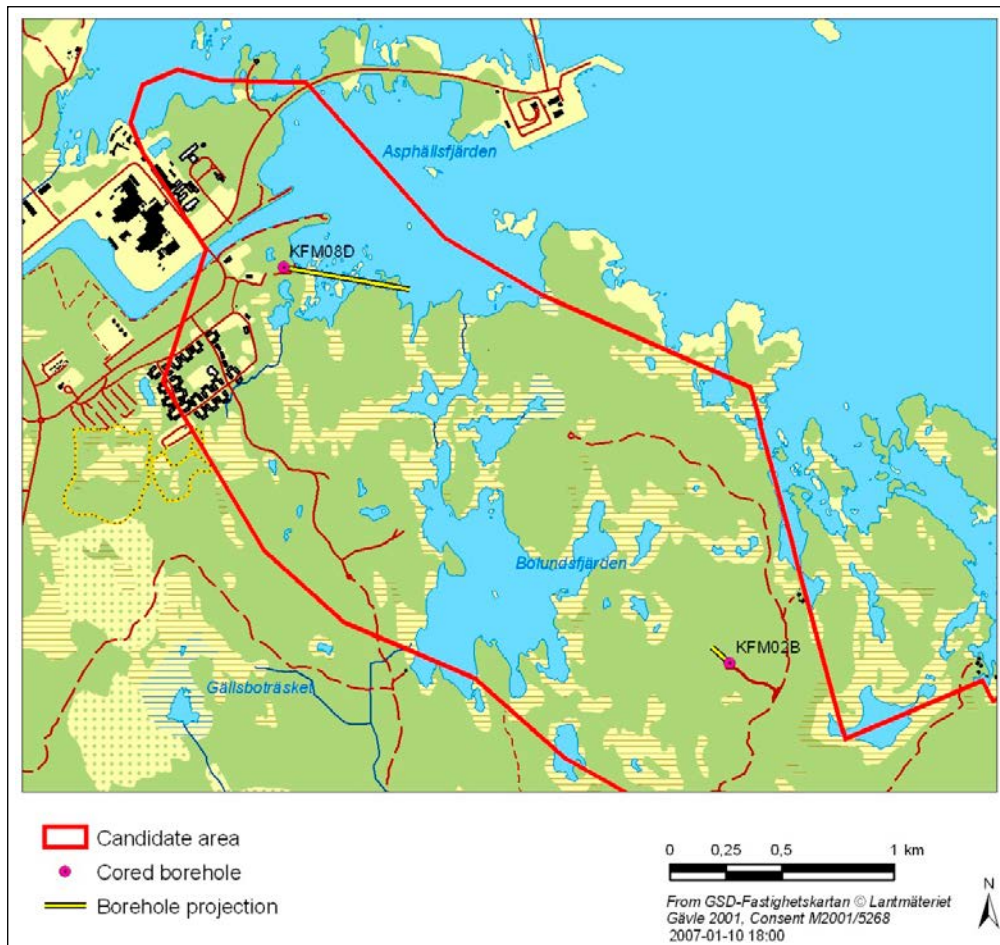
Figure 1-1. *Map of borehole location at the Forsmark investigation area.*

Original data from the reported activity are stored in the primary database Sicada. Data are traceable in Sicada by the Activity Plan number (AP SFK-10-069). Only data in databases are accepted for further interpretation and modelling. The data presented in this report are regarded as copies of the original data. Data in the databases may be revised, if needed. Such revisions will not necessarily result in a revision of the P-report, although the normal procedure is that major revisions entail a revision of the P-report. Minor revisions are normally presented as supplements, available at www.skb.se.

2 Objective and scope

Efforts to map the effects of the stress in the Forsmark region have been done with a suite of methods. This report describes a special processing of televiewer data with attention to the effect of stress: deformations of the borehole. The mapping is done according to the SKB-document AP SFK-10-069. An overview of the processed borehole is exposed in Table 2-1.

Table 2-1. Overview of boreholes (from Sicada).

Borehole	Length [m]	Inclination [° from hor.]	Orientation [° from GN]
KFM08D	942.3	−55.00	100.00

3 Equipment

The probe used for acquisition of data in 2014 is a BHTV sonde from Geovista Ltd., whereas in 2007 it was a High Resolution Acoustical Televiewer (HiRAT) from Robertson Geologging Ltd. The two probes are almost identical as they both are designed and built by Electromind.

The transducer is a 1.5 MHz head, which transmits the acoustic signal via a rotating acoustic mirror to the borehole wall. The strength of the reflected signal is recorded as an Amplitude log, while the first arrivals are picked and stored in a Traveltime log. Both logs are stored as images with selectable horizontal resolution from 90 to 360 pixels/revolution and a vertical resolution depending on the logging speed. The radial resolution in the recorded Traveltime is 100 nS, which equals 0.075 mm. The borehole was logged with same resoulution in both 2007 and 2014 as shown in Table 3-1.

The images are oriented by means of a built-in orientation unit containing a 3-axis fluxgate magnetometer as well a 3-axis accelerometer. The output from this device can also be used to calculate a deviation log for the borehole.

The probe is centralized in the borehole with two bow spring centralizers; see the picture in Figure 3-1. The applied centralizers are designated to boreholes with diameters in the range 67–100 mm.

Table 3-1. Overview of resolutions.

Borehole	Pixels/rev.	Horisontal res. [mm]	Logging speed [m/min.]	Vertical res. [mm]
KFM08D_2007	120	2.0	2.3	2
KFM08D_2014	120	2.0	2.3	2

Figure 3-1. *Picture of HiRAT probe.*

4 Processing of data

The final processing of the televiewer-data contains the steps described below. A lot of effort has been spent to investigate different possibilities in the processing. Only the final processing done to the delivered data is described. All processing is done in WellCAD, which is made by Advanced Logic Technology. A free reader for WellCAD documents can be downloaded on www.alt.lu.

4.1 Import and orientation

The televiewer data are recorded in the dedicated logging-program from Electromind. The data are stored in time domain, with a table which links the data to depth.

Image-data as well as orientation-data are imported and resampled to depth-domain. Orientation-data are filtered with a 25 samples moving average filter. Images are resampled to 360 pixels/rev. before orientation. This is done to prevent fractures from being edged during orientation.

Images are then oriented to Magnetic North (MN) by means of data from the orientation unit.

4.2 Alignment of images

In order to provide a system for length calibration of different logging systems used at the Forsmark site investigation, reference tracks (grooves) have been milled into the borehole wall with a specially designed tool at regular levels in all cored drilled boreholes. Regarding televiewer logging, the length calibration is conducted as follows.

First all BHTV logs are shifted, so that the upper edge of the top-most track is aligned to the milled reference track. Then all tracks in the borehole are identified and a table is made. The reference track marks in the borehole and the recorded track marks from the BHTV in borehole KFM08D are listed in Table 4-1.

Table 4-1. The reference track marks in the borehole and the recorded track marks form the BHTV in borehole KFM08D.

Reference mark [m]	HIRAT recorded [m]	Difference [m]
60.75	60.75	0.00
100.00	100.034	–0.03
150.00	150.082	–0.08
200.00	200.15	–0.15
250.00	250.19	–0.19
300.00	300.241	–0.24
350.00	350.301	–0.30
400.00	400.37	–0.37
450.00	450.426	–0.43
501.00	501.535	–0.54
550.00	550.631	–0.63
600.00	600.717	–0.72
650.00	650.799	–0.80
700.00	700.881	–0.88
750.00	751.027	–1.03
800.00	801.141	–1.14
850.00	851.223	–1.22
900.00	901.348	–1.35
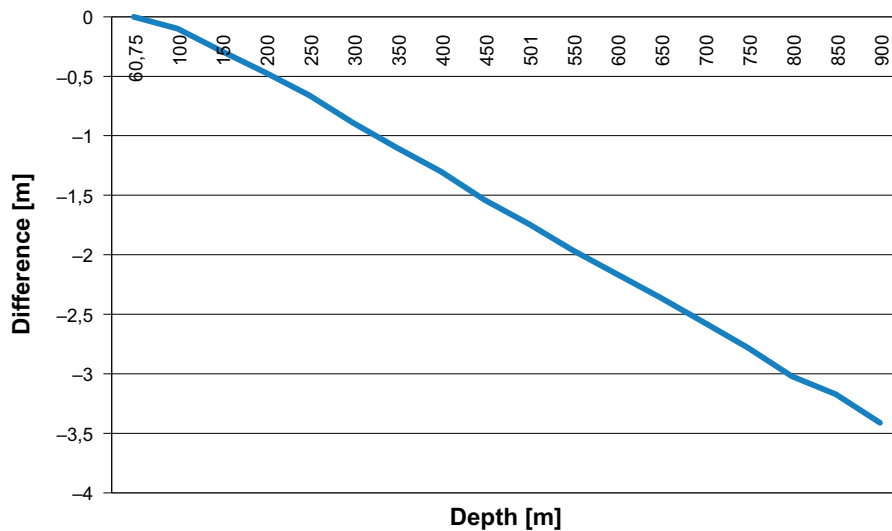
Figure 4-1. *Borehole KFM08D, plot of depth error.*

Also a plot of the differences is made. This is done to check the linearity of the depth error, an example of a plot is shown in Figure 4-1.

All logs are then stretched to fit the milled tracks in the borehole, which results in a perfect alignment to the tracks.

4.3 Filtering and calculation of decentralization

To calculate the decentralization, the Traveltime image needs to be filtered with a 15×15 pixels weighted average filter, which equals an area of 30×30 mm with 2×2 mm pixelsize. In boreholes with lower resolutions, the filter-size is reduced proportionally. This is done to prevent small fractures from disturbing the decentralization calculation. Then the image is converted from Traveltime (the unit is 100 nS) to radius with the formula:

$$Radius(mm) = \frac{(Travel\ Time - Internal\ Traveltime\ x\ 10)\ x\ VEL\ (FL)}{10\ x\ 1000} + tool\ radius$$

where "VEL(FL)" is the sound velocity in the borehole fluid

"Internal Traveltime" is the internal traveltime in the oil from the transducer to the acoustic window of the BHTV tool. As the sound velocity in the oil has a small temperature coefficient, it is calculated as:

$$Internal\ Traveltime = \frac{(-2.24\ x\ TEMP\ (FL) + 1031)\ x\ 120}{1000}$$

"TEMP(FL)" is the temperature of the water in the borehole, which was measured with a 9042 FluidRes and FluidTemp probe from Century Geophysical (see overview of acquisition reports in Appendix A). Also VEL(FL) is calculated in the report, from the measured resistivity of the fluid.

Next step is to extract statistics from the new radius image log, which returns logs for minimum, maximum, average and median values of the radius image. From these the decentralization of the probe is calculated as:

$$Decentralization = "Radius - mean" - "Radius - min"$$

4.4 Centralization of images

Due to the inclination of the boreholes, the acoustic televiewer-probe is slightly decentralized during logging; the size of this decentralization is roughly 0.1 mm/deg. from vertical. Therefore a centralization routine is applied to compensate the images for this. This is done by means of a sine-fitting routine in WellCAD. It can be done only to the Traveltime (Radius) image, not to the Amplitude image.

4.5 Calculation of calipers and ovality

The Centralized Traveltime is then also converted to a radius image as described in Section 4.3 and the previous image is deleted.

Now mean, minimum and maximum calipers as well as angles (eg. Caliper Max Position) for these can be extracted from the median filtered image log. Then the extracted angles (position logs) are filtered again with a 100 pts. (2 metre) moving average filter; this is done to smoothen the logs as only main angles are of interest.

An ovality log can now be calculated as twice the median radius minus the minimum caliper.

OVALITY – = "Radius – Centrelized – Median filtered – median" x 2 – "Caliper – min – Centralized – Median filtred"

This ovality log will only be reliable where some ovality is present, as it will be smeared by the fractures in the borehole as well as by method introduced artefacts. It also needs to be compared with the angle logs, which should be stable in one direction, before an eventual ovality can be considered reliable.

As a manual check of the ovality, cross-section logs are generated every 20 metres, as well as right above and below breakouts (the latter are deleted again). These cross-sections have grid-circles at every 0.5 mm, allowing the ovality to be visually checked, see example in Figure 4-2 below.

When necessary, the same process is applied to the downrun and imported to the uprun logpanel. It is used in case of doubt to help separating real deformations from artefacts. The Radius image is deleted again.

4.6 Registration of breakouts and other deformations

To register and describe deformations the log panel is manually inspected. When necessary, a cross-section is generated and the deformation, is classified, measured and registered in an Excel-table. In Figure 4-2 below an example of a cross-section is shown. The spacing between the radial grid here is 0.1 mm. The spikes on the cross-section, which have a maximum size of 0.3 mm, show some roughness on the borehole wall interpreted as micro fallout.

4.7 Nonconformities

The activity was performed in compliance with activity plan AP SFK-10-069.
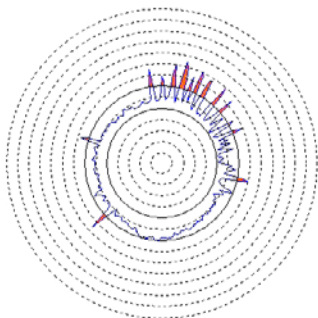
Figure 4-2. *Example of cross-section with micro fallout.*

5 Description of logpanel

5.1 Explanation of logs

Here follows – in alphabetic order – a description of all the logs in the panel.

5.1.1 Amplitude

Amplitude of the returned acoustic signal from the borehole wall. Darker (more blue) colours represent low amplitude – softer surface, while lighter (more yellow) colours represent high amplitude – harder surface of wall. The log is (as all other images) shown as an un-rolled 360° image of the borehole, where 0° is the reference, which is aligned against magnetic north (MN). The image has no unit.

5.1.2 Caliper max position

Orientation of the calculated maximum caliper in degrees from MN of the borehole. The log is derived from the filtered and centralized radius image. Contains values from 0–180 degrees.

5.1.3 Caliper min position

Orientation of the calculated minimum caliper in degrees from MN of the borehole. The log is derived from the filtered and centralized radius image. Contains values from 0–180 degrees.

5.1.4 Caliper – max – Centralized – Median filtered

Maximum caliper measured in the median filtered and centralized radius image. Unit: mm.

5.1.5 Caliper – mean – Centralized – Median filtered

Mean caliper measured in the median filtered and centralized radius image. Unit: mm.

5.1.6 Caliper – min – Centralized – Median filtered

Minimum caliper measured in the median filtered and centralized radius image. Unit: mm.

5.1.7 Class

Symbol log, which shows the classification of registered deformations. This log is pasted from the column in the registration Excel-sheet.

BB		Borehole Breakout
KS		Key Seat
MF		Micro Fallout
WO		Washout

5.1.8 Cross-section – Radius – Centralized

Cross-sections are generated every 20 metres in the borehole. The cross-section is average over 10 cm. Radii below the actual nominal radius are shaded green, and radii above are shaded orange.

5.1.9 Decentralization

Calculated decentralization as the difference between the mean and min radius of the radius image. Unit: mm.

5.1.10 Radius – Centralized

Radius image log, which is centralized as described to compensate for decentralization of the probe. Light colours represent smaller radii, while darker colours represent larger radii. Unit: mm.

5.1.11 Radius – Centralized – Median filtered

Radius image log, which is centralized as described earlier and median filtered over an area of 15×15 pixels (app. 20×30 mm) to shade for small deformations, when calculating calipers. Light colours represent smaller radii, while darker colours represent larger radii. Unit: mm.

5.1.12 Radius – Centralized – Median filtered – median

This log is not shown; it is used to calculate the ovality as described in paragraph 4.5.

5.1.13 Radius – Median filtered – max

Maximum radius of the median filtered, but not centralized radius image, unit: mm.

5.1.14 Radius – Median filtered – median

Median radius of the median filtered, but not centralized radius image, unit: mm.

5.1.15 Radius – Median filtered – mean

Mean radius of the median filtered, but not centralized radius image, unit: mm.

5.1.16 Radius – Median filtered – min

Minimum radius of the median filtered, but not centralized radius image, unit: mm.

5.1.17 Tool rotation

Shows the rotation of the probe, as the borehole was logged, unit: degrees.

6 Analysis and registration of observed deformations

6.1 Classification of observed deformations

In Appendix C tables with classification of all interpreted deformations in borehole KFM08D are presented The classification is illustrated in Figure 6-1.

6.2 Explanation of columns in the Excel-sheet

The columns in the Excel-sheet are explained as follows:

Top Depth: Top of the deformation.

Bot. Depth: Bottom of the deformation.

Max. R: Maximum radius of the deformation, read from "Radius – max – Median Filtered"-log and/ or "Radius" image.

Median R: Nominal radius at the depth, read from "Radius – median – Median Filtered"-log.

dRmax: Delta radius, i.e. the depth of the deformation into the borehole wall.

Structure: Classification of the deformation. Examples and further explanation are shown in paragraph 6.3:
    BB: Borehole breakout.
    WO: Washout.
    KS: Key seat.
    MF: Micro fallout.

Uncertainty: The uncertainty of the observed deformation: 3 = certain, 2 = probable, 1 = possible, 0 = not estimated. The uncertainty is primary related to the type of deformation.

Cross. struct.: The deformation is related to a fracture crossing the borehole. Example of this is shown in paragraph 6.3.

Main azimuth: Main azimuth of the deformation in degrees from Magnetic North. The angle is calculated from the next column "Azimuth". If the angle is between 0 and 180°, the main azimuth is the same, but if the azimuth is between 180 and 360°, 180° are subtracted from the angle. Example of this is shown and explained in paragraph 6.3.

Azimuth: Angle from MN to the dominating point of the deformation.

Apertureα1: Angle from MN to first edge of the deformation. If the deformation is located around 0° MN, this angle is noted as a negative angle from MN, e.g. –5°. This angle equals 355°.

Apertureα2: Angle from MN to last edge of the deformation.
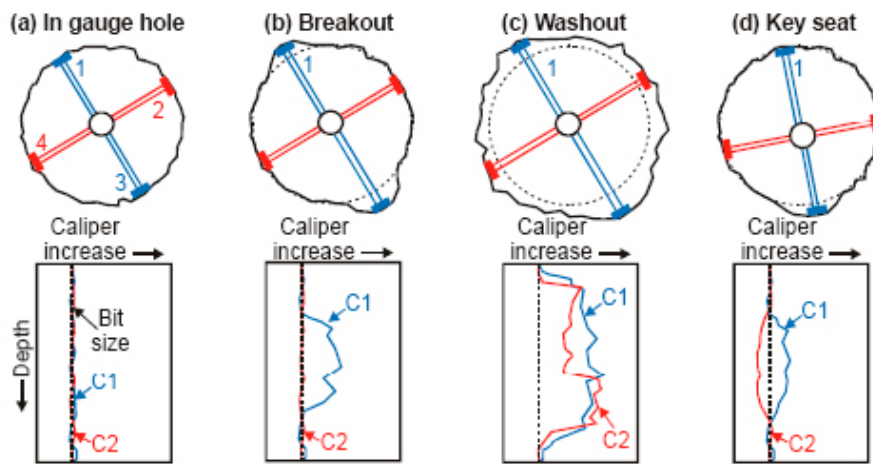
Angles described above are illustrated in Figure 6-2.

Figure 6-1. *Classification of deformations (from Ask and Ask 2007, after Plumb and Hickman 1985).*
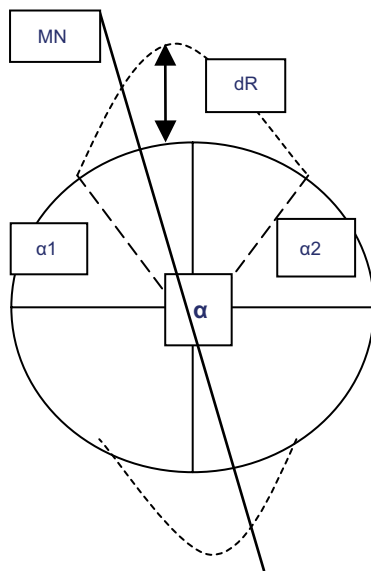

Figure 6-2. *Illustration of angles.*

6.3 Examples of borehole deformations

6.3.1 Example of borehole breakout (BB)

In Figure 6-3 an example of borehole breakouts from KFM07C is shown. As there are obvious diametrically opposite deep fallouts, this deformation is Classified as BB with the uncertainty as "3" – most certain. As the breakout is seen to be in connection with a fracture crossing the borehole, a "Y" (Yes) is placed in the "Crossing structure" column. Here the deepest and most dominating fallout is seen at 50° and the aperture of the fallout is read to be from 0 to 100°.

The centralization routine is only perfect in a truly circular borehole. Elsewhere it adds some distortion to the centralized images, which can be seen as white (closer) areas around the fallouts. Therefore the truest picture of fallouts is seen on the "Radius"-image and the "Amplitude"-image, as these are not centralized.

6.3.2 Example of washout (WO)

In Figure 6-4 an example of washout (WO) from KFM07C is shown. Washouts are separated from breakouts, as there is fallout in the entire perimeter of the borehole, thus the minimum diameter is enlarged. Also here (if possible) a dominating azimuth and aperture angles are read and registered in the Excel sheet.
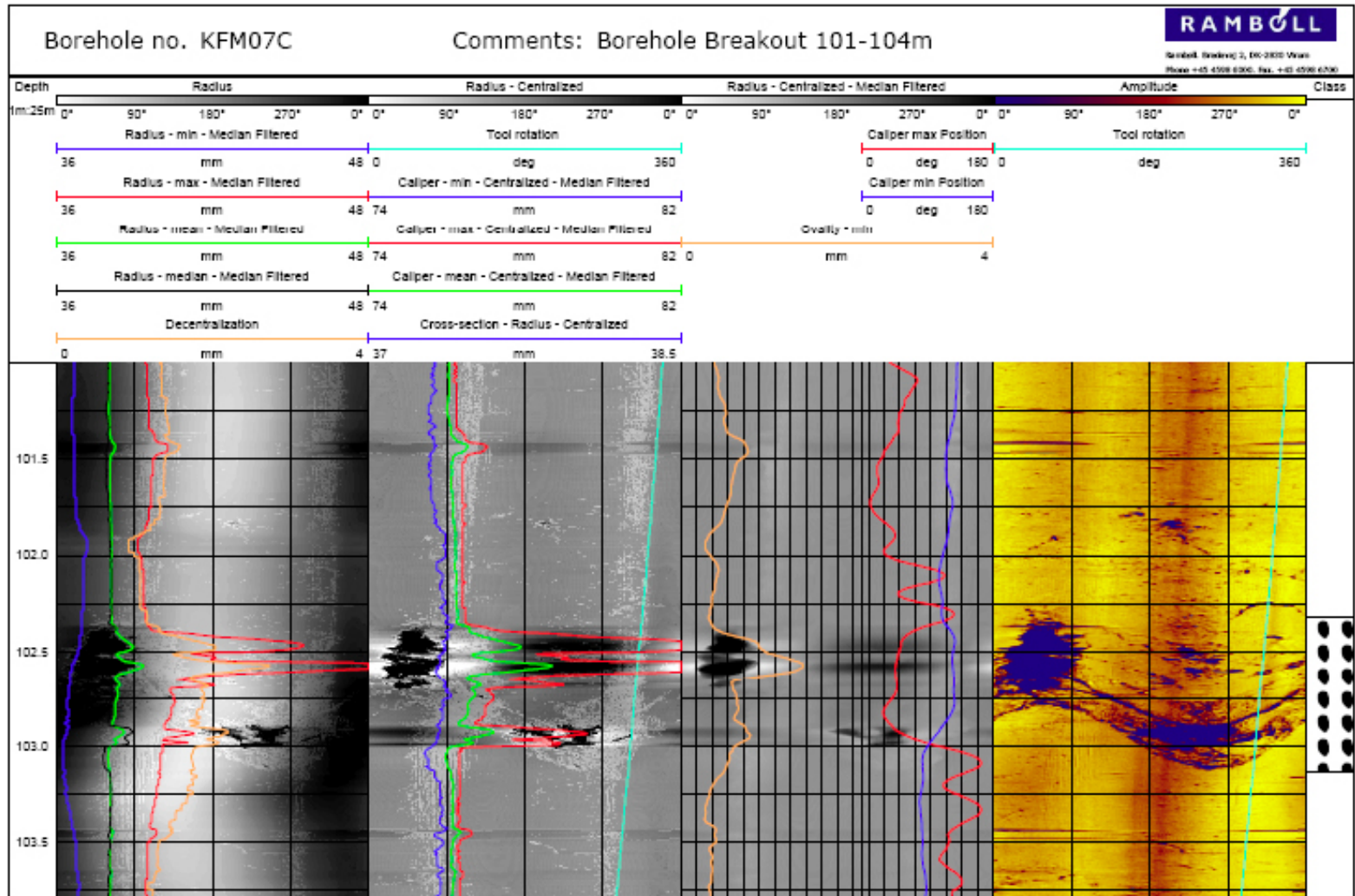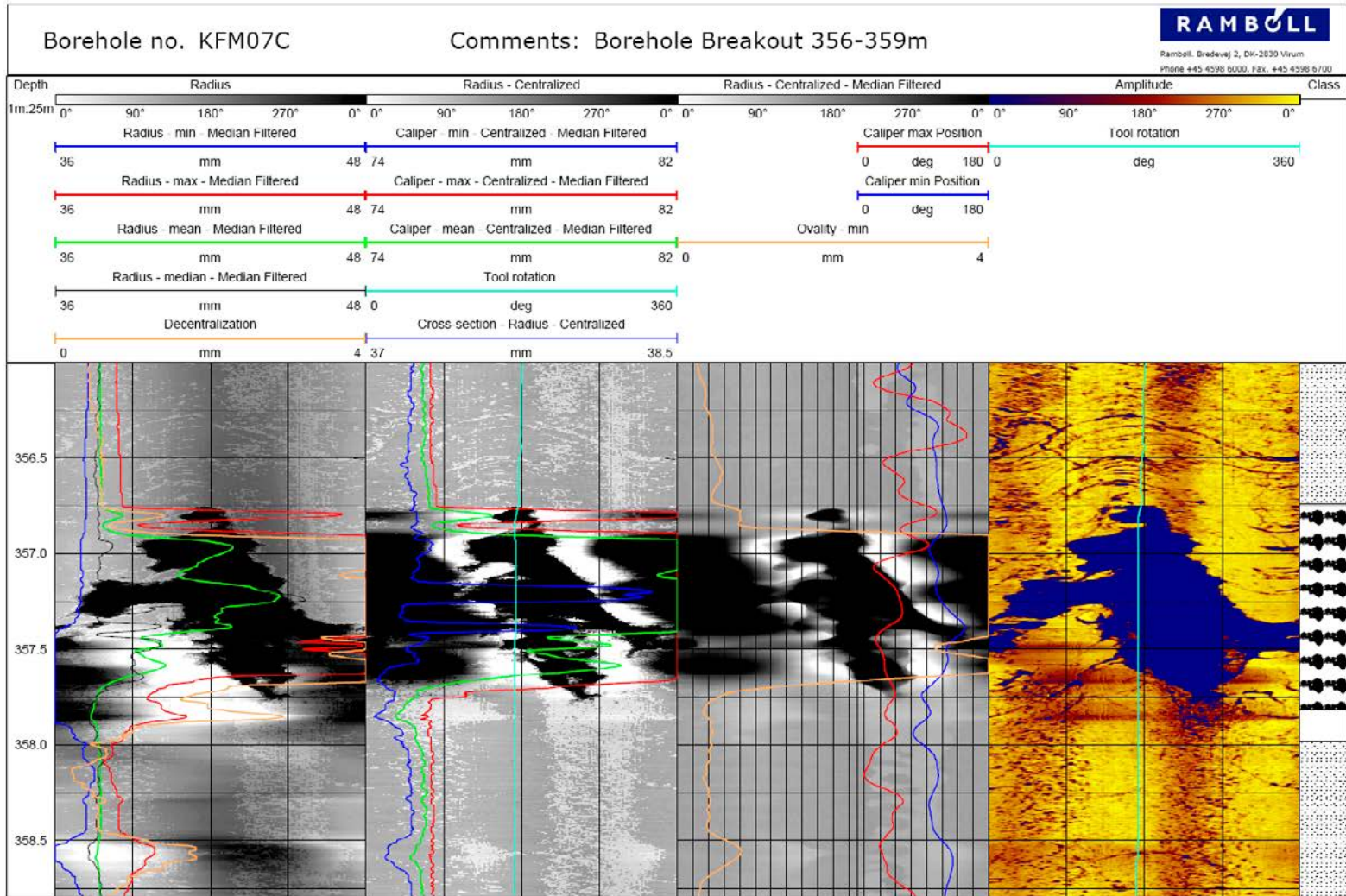
Figure 6-3. *Example of borehole breakout from KFM07C.*

Figure 6-4. *Example of washout from KFM07C.*

6.3.3 Example of keyseat (KS)

In Figure 6-5 an example of a keyseat (KS) from KFM07C is displayed. The keyseat is recognised as fallout in only one direction at the relevant depth. Also here azimuth and aperture angles are read and registered in the Excel sheet.

6.3.4 Example of micro fallout (MF)

In Figure 6-6 an example of micro fallout is presented. In this example the micro fallout is recognized as two verticals bands in the borehole (which here ends at 205 m). In these cases azimuth and aperture angles are registered. In other cases the fallout is found in the entire circumference of the borehole (with or without a dominating azimuth). In these cases the aperture angles are registered as 0 to 360°.

The micro fallout is mainly recognised on the Amplitude-image. It is sometimes hard to separate from breakouts, but a condition has been set up, that breakouts should be found also on the Radius-images as darker areas – holes. The registration of micro fallout is generally the most uncertain.

6.4 Explanation of special features in the boreholes

6.4.1 Tracks from decentralization

In Figure 6-7 a section from KFM01B with different kinds of tracks and shadows found in the boreholes is shown.

- On the Amplitude image dark tracks are seen which follow the rotation of the tool. These tracks have an internal spacing of 90° and come from the centralizers on the acoustic televiewer probe. This is confirmed by the downrun log, on which they are not present.

- The rotation introduces a slight decentralization of the tool, which also follows the rotation. The remedy of the decentralization is explained in the paragraph regarding processing, but it still leaves some darker bands on the images. These darker bands, which follow the tool rotation, are artificial.

- Furthermore some vertical tracks are observed on both the amplitude- and radius-images. They are anticipated to have been made by centralizers from other probes, e.g. the BIPS-probe. In parts of the borehole, they are also recognised on the BIPS-image (Gustafsson and Gustafsson 2004).

6.4.2 Drill cuttings from bottom of borehole

In Figure 6-8 an example from the bottom of KFM01B is presented. Here drill cuttings from the bottom of the hole have partly covered the acoustic window, but is slowly washed off.

6.4.3 Wobbles from drilling process

In Figure 6-9 an example of "wobbles" made by the drilling process is displayed. These wobbles are frequently seen in the boreholes and in some cases they make it hard to register deformations in these areas.
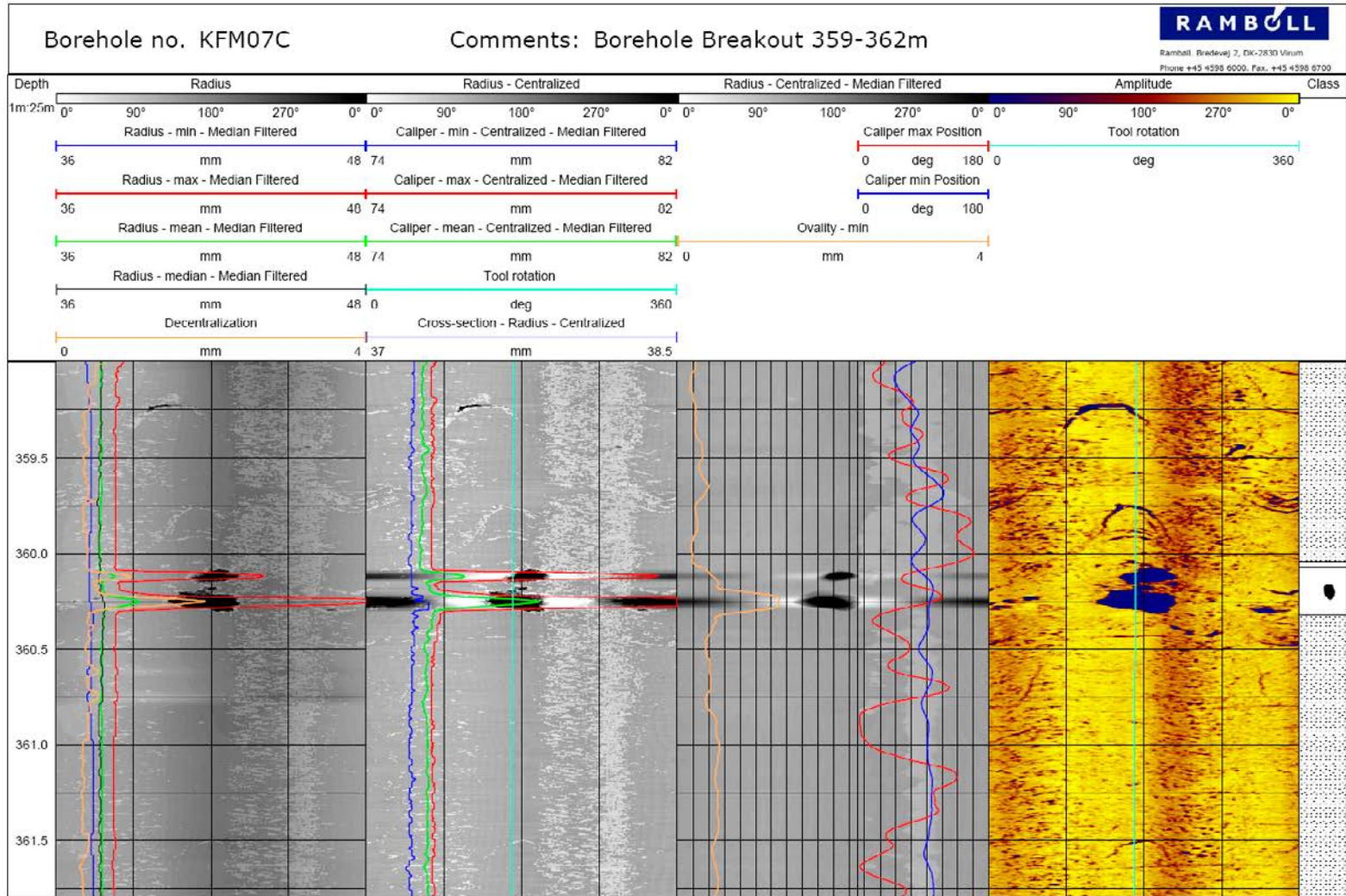
Figure 6-5. *Example of keyseat from KFM07C.*
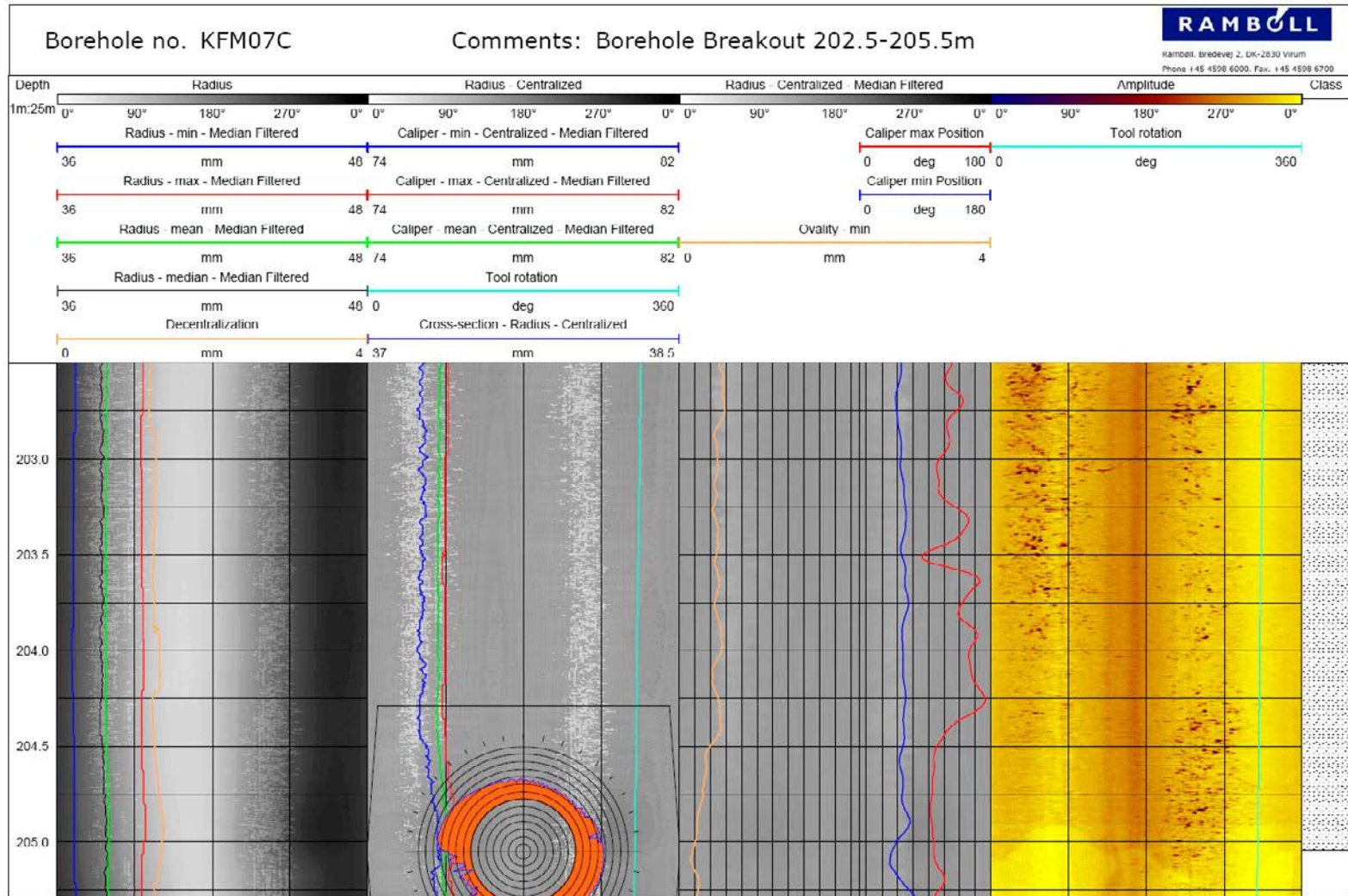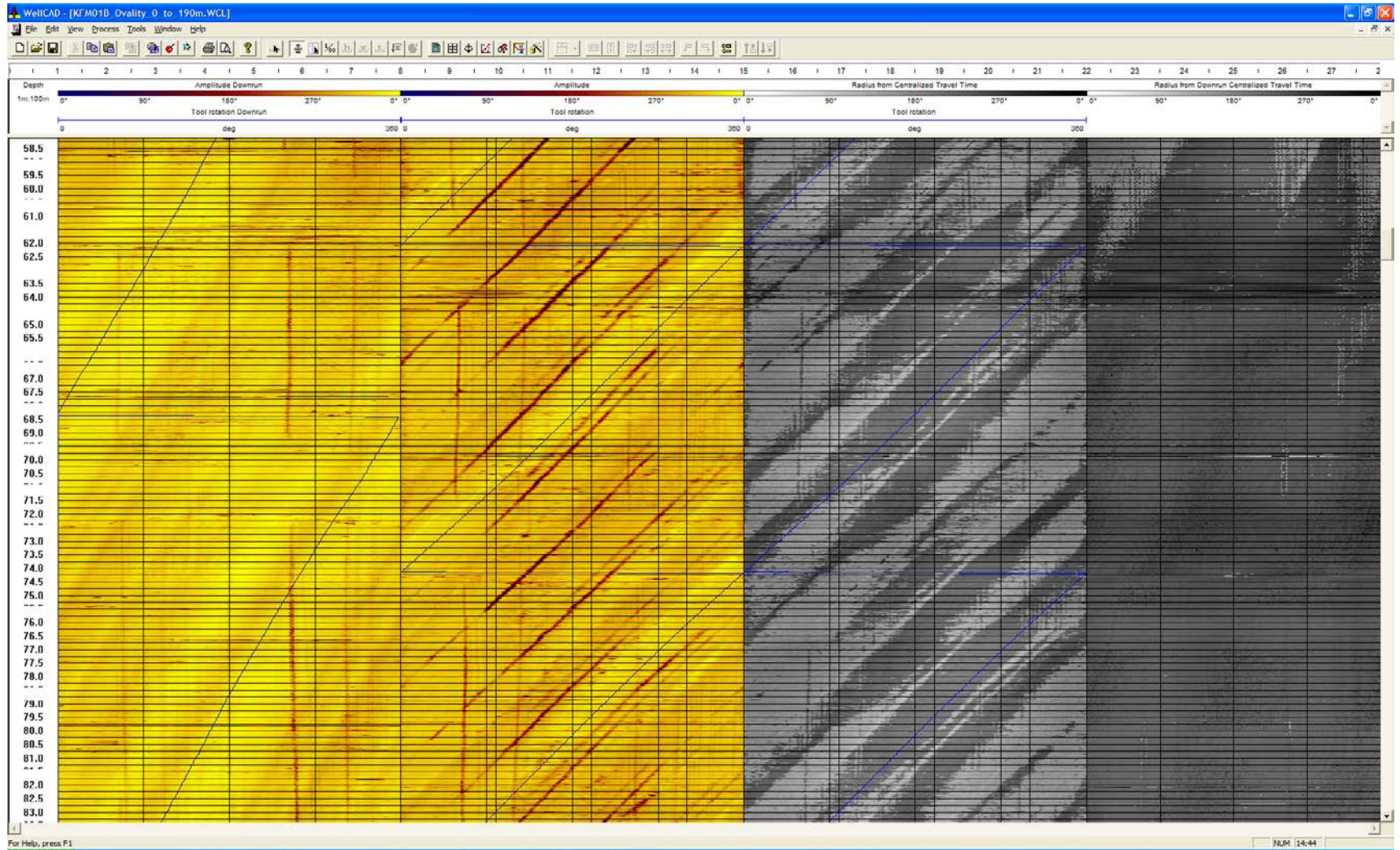
Figure 6-6. *Example of micro fallout from KFM07C.*

Figure 6-7. *Example of tracks and shadows from KFM01B, 58.5 to 83 m.*

Figure 6-8. *Example of drill cuttings on the acoustic window.*
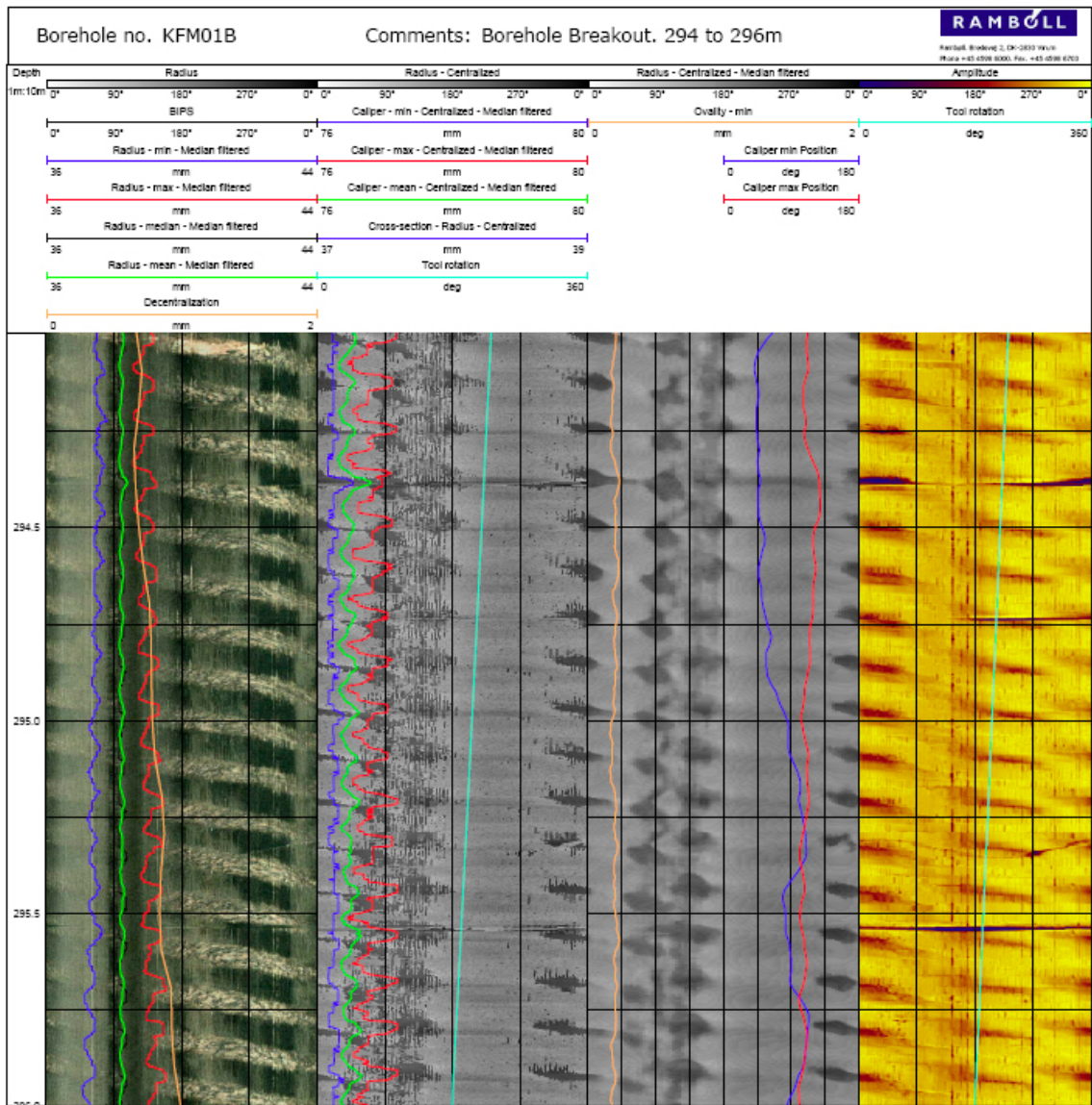
Figure 6-9. *Example of wobbles.*

7 KFM08D Breakout processing

In an effort to conclude whether breakouts caused by the stress field has a momentary character, as the drillhole is made, or is an ongoing, time dependent process, KFM08D has been surveyed twice with the acoustic televiewer. The first televiewer survey in KFM08D was performed on 2007-02-20 (1 week after the drilling was finished), the second was done in January 2014, i.e. 7 years later.

7.1 Time dependence of breakout

The deformations registered in KFM08D are shown in Table 7-1.

As seen, the same registered deformations are registered in both surveys to a depth of 924 m.

All data is registered in an Excel spreadsheet: "KFM08D_Breakout_Evaluation_2007–2014_Rev1. xls", and then digitally copied to the "Class" track in the WellCAD documents. The spreadsheet contains data from both the 2007 and 2014 surveys.

The images from the two surveys have been manually inspected side-by-side in a display.

There are no signs of any difference in the breakout registration seen above a depth of 924 m. From 924 m to 927 m (close to the borehole bottom) many breakouts are registered. There are maybe some time dependent breakouts seen in the 2014 survey at the depths 924.28 m, 925.6 m and 926.3 m. The interval is shown in Figure 7-1 with the features marked.

Table 7-1. Registered deformations in KFM08D to a depth of 924 m.

Class	2007	2014
BB	10	10
WO	0	0
KS	12	12
MF	5	5
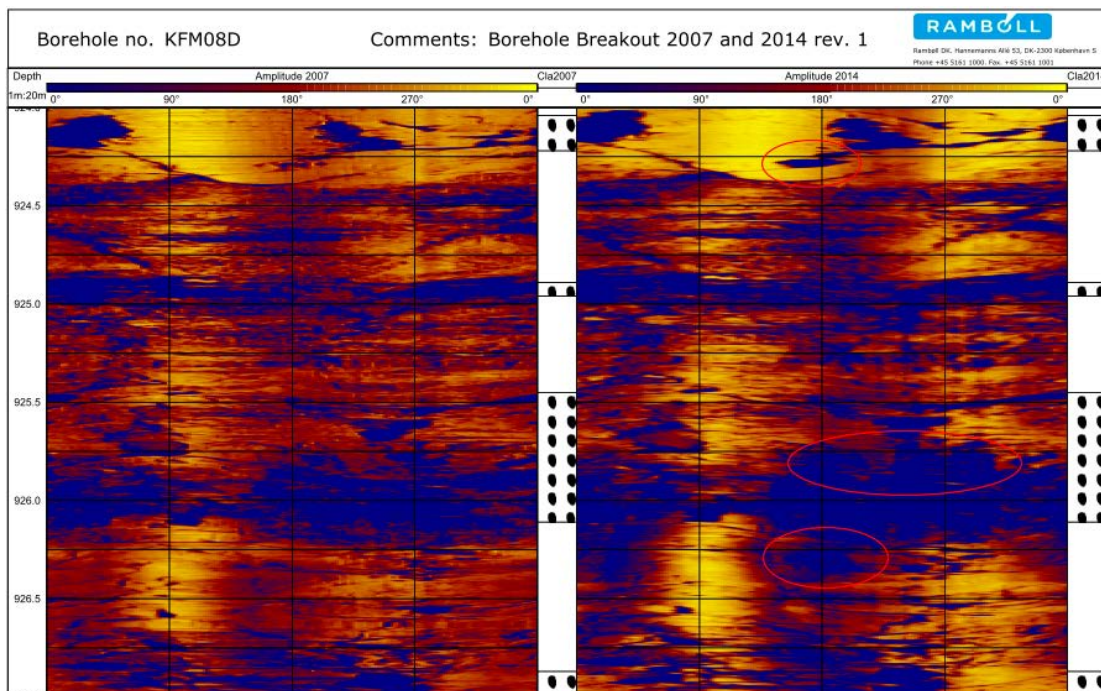
***Figure 7-1.** Change of the borehole surface from 2007 to 2014. Interval 924–927 m.*

Some other features not registered as breakouts are seen within two depth intervals, 200.9–201.3 m, shown in Figure 7-2, and 392.9–393.3 m, shown in Figure 7-3. The features seen in Figure 7-2 cannot be explained, whereas the feature seen in Figure 7-3 may represent water inflow to the borehole.
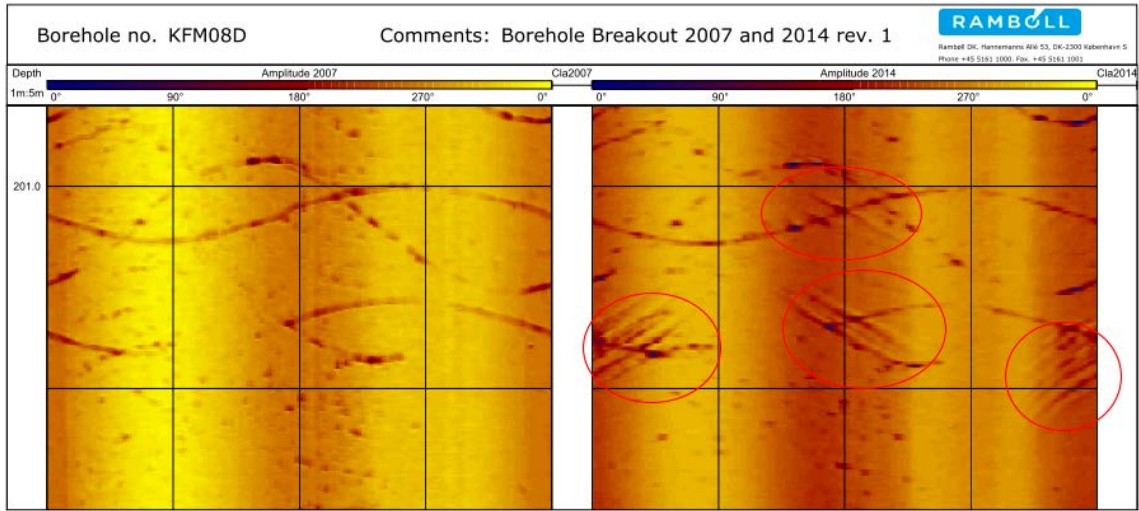
Figure 7-2. *Change of the borehole surface from 2007 to 2014. Interval 200.9–201.3 m.*
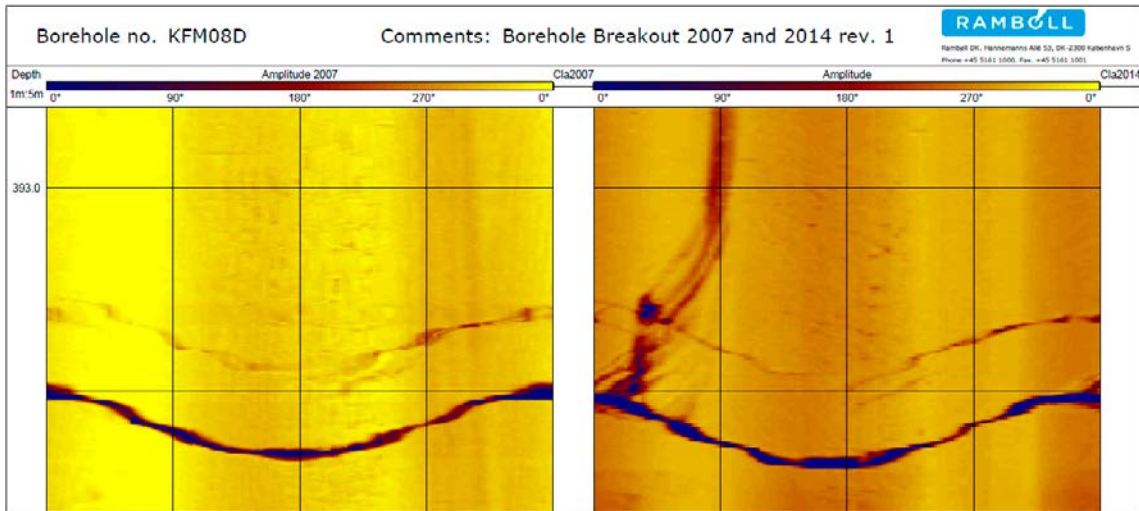
Figure 7-3. *Possible water inflow. The 2007 results are found to the left and the 2014 results to the right. Interval 392.9–393.3 m.*

8 Summary and discussions

- It does not take long to locate larger deformations, simply by means of scrolling through a calculated high resolution caliper.

- Orientation and size of the deformations can be precisely mapped.

- From the study of the two surveys in KFM08D with 7 years interval, it is concluded that no time dependent deformations has taken place in this borehole above 924 m.

- In boreholes deviated more the 10° from vertical, the cross-sections are often too disturbed of noise from decentralization to be used.

- It is strongly recommended, that the logpanels are evaluated in WellCAD or the free WellCAD-reader, as a print-out or PDF does not provide the necessary flexibility to zoom and focus on relevant deformations.

- When smaller breakouts or micro fallouts are found in connection with fractures, it can be difficult to clarify, whether the fallout was caused by the drilling process or by stress.

References

SKB's (Svensk Kärnbränslehantering AB) publications can be found at www.skb.se/publications.

Ask D, Ask M V S, 2007. Forsmark site investigation. Detection of potential borehole breakouts in boreholes KFM01A and KFM01B. SKB P-07-235, Svensk Kärnbränslehantering AB.

Ask M V S, Ask D, Christiansson R, 2006. Detection of borehole breakouts at the Forsmark site, Sweden. In Lu M, Li CC, Kjørholt H, Dahle H (eds). In-situ rock stress: measurement, interpretation and application: proceedings of the International Symposium on In-situ Rock Stress, Trondheim, Norway, 19–21 June, 2006. London: Taylor and Francis, 79–86.

Deltombe J-L, Schepers R, 2000. Combined processing of BHTV traveltime and amplitude images. In Proceedings of International Symposium on Borehole Geophysics for Minerals, Geotechnical, and Groundwater Applications, Denver, Colorado. Houston, TX: The Minerals and Geotechnical Logging Society, Vol. 7, 29–42.

Gustafsson J, Gustafsson C, 2004. Forsmark site investigation. RAMAC and BIPS logging in borehole KFM01B and RAMAC directional re-logging in borehole KFM01A. SKB P-04-79, Svensk Kärnbränslehantering AB.

Plumb R A, Hickman S H, 1985. Stress-induced borehole elongation: a comparison between four-arm dipmeter and the borehole televiewer in the Auburn geothermal well. Journal of Geophysical Research 90, 5513–5521.

Ringgaard J, 2007. Mapping of borehole breakouts. Processing of acoustical televiewerdata from KFM01A, KFM01B, KFM02A, KFM03A, KFM03B, KFM04A, KFM05A, KFM06A and KFM07C. SKB P-07-07, Svensk Kärnbränslehanteing.

Zoback M D, Moos D, Mastin L, Anderson R N, 1985. Well bore breakouts and in situ stress. Journal of Geophysical Research 90, 5523–5530.

List of acquisition reports

List of acquisition reports from logging with acoustic televiewer, fluid temperature and resistivity – and calculation of fluid velocity.
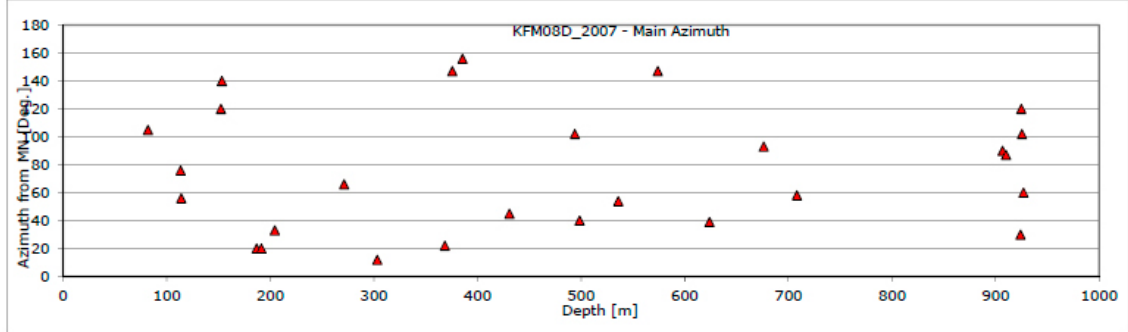
KFM08D: **Nielsen U T, Ringgaard J, 2007.** Forsmark site investigation. Geophysical borehole logging in boreholes KFM02B and KFM08D. SKB P-07-60, Svensk Kärnbränsle-hantering AB.

Tables and charts of registered deformations

B1   KFM08D. February 2007

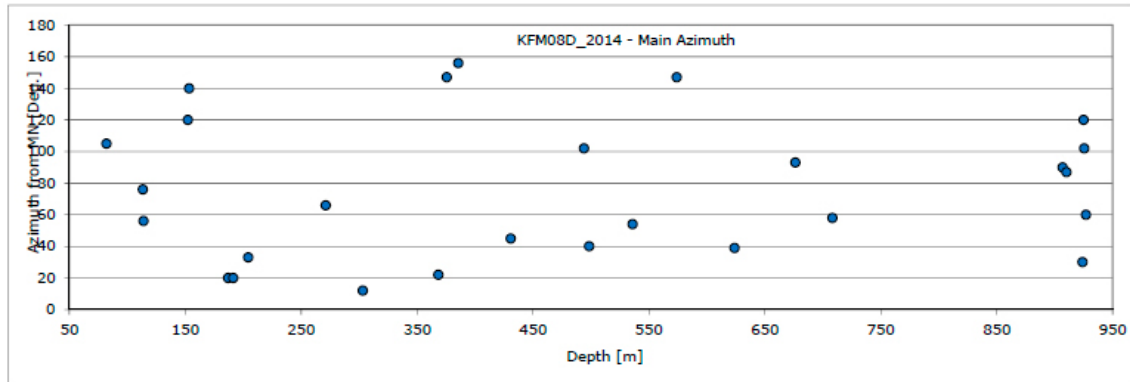**KFM08D_2007 - Observed BB, WO, MF and KS.**

Top Depth	Bot. depth	Class	Uncertaint	Cross. struct	Main Azimuth	Azimuth	Aperture a1	Aperture a2	Comments
[m]	[m]		[0-3]	[Yes/No]	[Deg. from MN]	[Deg. from MN]	[Deg. from MN]	[Deg. from MN]	
81.98	82.04	KS	2	Y	105	285	270	302	
113.47	113.77	BB	3	Y	76	76	50	110	
113.94	114.07	BB	2	Y	56	56	26	86	
152.25	152.39	KS	1	Y	120	120	112	130	
153.27	153.32	KS	1	Y	140	140	124	156	
186.93	187.46	BB	1	Y	20	20	6	38	
191.34	191.63	MF	2	Y	20	200	0	360	
204.33	205.73	MF	1	Y	33	213	150	228	
271.12	271.51	KS	3	Y	66	66	56	76	
303.21	303.34	MF	2	N	12	192	180	201	
368.41	368.48	BB	1	Y	22	22	12	40	
375.63	376.30	MF	1	Y	147	147	129	171	
385.49	385.91	KS	2	Y	156	156	145	185	
430.87	431.06	KS	2	Y	45	45	-15	54	
494.01	494.50	BB	1	Y	102	282	183	309	
498.42	498.62	KS	2	Y	40	220	190	250	
535.92	536.33	KS	1	Y	54	234	224	246	
573.97	574.38	MF	2	Y	147	147	108	213	
623.86	624.32	KS	1	Y	39	39	3	51	
676.19	676.37	KS	3	Y	93	273	225	330	
708.23	708.47	BB	3	N	58	58	34	94	
906.81	907.36	KS	2	Y	90	85	39	147	
910.18	910.26	KS	2	Y	87	87	75	93	
924.04	924.22	BB	3	Y	30	30	-15	57	
924.89	924.96	BB	3	Y	120	300	266	334	
925.45	926.11	BB	3	y	102	282	0	360	
926.87	927.10	BB	3	Y	60	240	210	266	

B2   KFM08D. January 2014

KFM08D_2014 - Observed BB, WO, MF and KS.

Top Depth	Bot. depth	Class	Uncertaint	Cross. struct	Main Azimuth	Azimuth	Aperture α1	Aperture α2	Comments
[m]	[m]		[0-3]	[Yes/No]	[Deg. from MN]	[Deg. from MN]	[Deg. from MN]	[Deg. from MN]	
81.98	82.04	KS	2	Y	105	285	270	302	
113.47	113.77	BB	3	Y	76	76	50	110	
113.94	114.07	BB	2	Y	56	56	26	86	
152.25	152.39	KS	1	Y	120	120	112	130	
153.27	153.32	KS	1	Y	140	140	124	156	
186.93	187.46	BB	1	Y	20	20	6	38	
191.34	191.63	MF	2	Y	20	200	0	360	
204.33	205.73	MF	1	Y	33	213	150	228	
271.12	271.51	KS	3	Y	66	66	56	76	
303.21	303.34	MF	2	N	12	192	180	201	
368.41	368.48	BB	1	Y	22	22	12	40	
375.63	376.30	MF	1	Y	147	147	129	171	
385.49	385.91	KS	2	Y	156	156	145	185	
430.87	431.06	KS	2	Y	45	45	-15	54	
494.01	494.50	BB	1	Y	102	282	183	309	
498.42	498.62	KS	2	Y	40	220	190	250	
535.92	536.33	KS	1	Y	54	234	224	246	
573.97	574.38	MF	2	Y	147	147	108	213	
623.86	624.32	KS	1	Y	39	39	3	51	
676.19	676.37	KS	3	Y	93	273	225	330	
708.23	708.47	BB	3	N	58	58	34	94	
906.81	907.36	KS	2	Y	90	85	39	147	
910.18	910.26	KS	2	Y	87	87	75	93	
924.04	924.22	BB	3	Y	30	30	-15	57	
924.89	924.96	BB	3	Y	120	300	266	334	
925.45	926.11	BB	3	y	102	282	0	360	
926.87	927.10	BB	3	Y	60	240	210	266	

Plot of logpanels